

A Novel Neutrophil-Specific PET Imaging Agent: cFLFLFK-PEG-⁶⁴Cu

Landon W. Locke¹, Mahendra D. Chordia², Yi Zhang³, Bijoy Kundu³, Dylan Kennedy⁴, Jessica Landseadel⁵, Li Xiao³, Karen D. Fairchild⁵, Stuart S. Berr^{1,3}, Joel Linden⁴, and Dongfeng Pan³

¹Department of Biomedical Engineering, University of Virginia, Charlottesville, Virginia; ²Department of Chemistry, University of Virginia, Charlottesville, Virginia; ³Department of Radiology, University of Virginia, Charlottesville, Virginia; ⁴Cardiovascular Research Center, University of Virginia, Charlottesville, Virginia; and ⁵Department of Pediatrics, University of Virginia, Charlottesville, Virginia

The synthesis and validation of a new, highly potent ⁶⁴Cu-labeled peptide, cFLFLFK-PEG-⁶⁴Cu, that targets the formyl peptide receptor (FPR) on leukocytes is described. The peptide ligand is an antagonist of the FPR, designed not to elicit a chemotactic response resulting in neutropenia. Evidence for the selective binding of this synthesized ligand to neutrophils is provided. PET properties of the compound were evaluated in a mouse model of lung inflammation. **Methods:** The FPR-specific peptide, cinnamoyl-F-(D)L-F-(D)L-FK (cFLFLF), was sequentially conjugated with a bifunctional polyethylene glycol moiety (PEG, 3.4 kD) and a 2,2',2''-(1,4,7,10-tetraazacyclododecane-1,4,7,10-tetrayl)tetraacetic acid (DOTA) through a lysine (K) spacer and finally labeled with ⁶⁴Cu-CuCl₂ to form cFLFLFK-PEG-⁶⁴Cu. The binding affinity and stimulation potency of the ligand toward human neutrophils were assessed in vitro. Blood kinetic and organ biodistribution properties of the peptide were studied in the mouse. Ten male C57BL/6 mice were used in this study; 4 control mice and 6 administered *Klebsiella pneumoniae*. PET/CT scans were performed to assess the localization properties of the labeled peptide in lungs 18 h after tracer administration. Lung standardized uptake values (SUVs) were correlated with lung neutrophil activity as measured by myeloperoxidase assays. Immunohistochemistry was performed to confirm that neutrophils constitute the majority of infiltrating leukocytes in lung tissue 24 h after *Klebsiella* exposure. **Results:** In vitro binding assays of the compound cFLFLFK-PEG-⁶⁴Cu to the neutrophil FPR yielded a dissociation constant of 17.7 nM. The functional superoxide stimulation assay exhibited negligible agonist activity of the ligand with respect to neutrophil superoxide production. The pegylated peptide ligand exhibited a blood clearance half-life of 55 ± 8 min. PET 18 h after tracer administration revealed mean lung SUVs and lung myeloperoxidase activities for *Klebsiella*-infected mice that were 5- and 6-fold higher, respectively, than those for control mice. Immunohistochemistry staining confirmed that the cellular infiltrate in lungs of *Klebsiella*-infected mice was almost exclusively neutrophils at the time of imaging. **Conclusion:** This new radiolabeled peptide targeting the FPR binds to neutrophils in vitro and accumulates at sites of inflammation in vivo. This modified peptide may prove to be a useful tool to probe inflammation or injury.

Key Words: PET; neutrophils; FPR antagonist; inflammation imaging; molecular imaging

J Nucl Med 2009; 50:790-797

DOI: 10.2967/jnumed.108.056127

Tissue damage caused by trauma, infection, or other stimuli triggers a complex sequence of events collectively known as the inflammatory response. This response includes the directed migration of neutrophils from circulation to the site of injury with the ultimate goal of killing pathogens. Although inflammation is critical to survival, exaggerated or persistent inflammation causes collateral damage that plays a key role in the progression of many major diseases. Neutrophils are among the first leukocytes to reach a site of injury, and they are abundant at focal sites of infection (1). The ability to detect and quantify neutrophilic accumulation could be important not only in locating and identifying inflammatory lesions but also in facilitating the development and testing of antiinflammatory agents.

Currently available clinical nuclear imaging probes for targeting and diagnosing inflammatory lesions include ⁶⁷Ga citrate and ¹¹¹In or ^{99m}Tc leukocytes labeled ex vivo (2). Although each of these agents can yield useful results in specific situations, each possesses significant drawbacks. In general, techniques using in vitro labeling of white blood cells suffer the disadvantage of lengthy, laborious, and potentially hazardous labeling procedures. In contrast, injection of peptides that have a high affinity for surface receptors on leukocytes has emerged as an attractive option for the in vivo detection of inflammation. Formyl peptides, synthetic analogs of natural bacteria products, have been extensively studied as a possible replacement for current techniques for imaging inflammation. Because peptide probes specifically target leukocytes in vivo, the disadvantages associated with ex vivo laboratory labeling procedures are avoided. Although prior studies have shown promising results detecting leukocyte accumulation in response to inflammatory stimuli with peptide probes in vivo,

Received Jul. 18, 2008; revision accepted Oct. 28, 2008.

For correspondence or reprints contact: Dongfeng Pan, Department of Radiology, University of Virginia, Box 801339, Charlottesville, VA, 22908.

E-mail: dp3r@virginia.edu

COPYRIGHT © 2009 by the Society of Nuclear Medicine, Inc.

several problems remain. For example, some of these peptides are potent receptor agonists, with the potential for causing neutrophil activation and neutropenia at high doses (3). Several ^{99m}Tc - and ^{111}In -labeled chemotactic peptide ligands including agonist formyl-methionyl-leucyl-phenylalanine (fMLF) (4,5) and the antagonist *i*-Boc-MLF (6) have been investigated for imaging inflammation *in vivo*. fMLF-based agonist ligands have high affinity for neutrophils; however, they were found to induce chemotaxis, cell adhesion, and degranulation of leukocytes; responses associated with infection and inflammation (7). On the other hand, *i*-Boc-MLF did not exhibit undesirable neutrophil-activating effects but exhibited weak binding affinity. An ideal imaging peptide ligand to detect neutrophilic inflammation would exhibit high binding affinity for neutrophils and could be used at doses less than their binding dissociation constant (K_d) without significantly perturbing their function or influencing their distribution.

The peptide cinnamoyl-F-(D)L-F-(D)L-F (cFLFLF) was reported as an antagonist to the neutrophil FPR with a high binding affinity ($K_d = 2 \text{ nM}$) (3). However, because of its high hydrophobicity it demonstrated relatively poor target-to-background ratios, compared with peptide agonists, in imaging focal sites of infection in rabbits. To address this problem, we modified the peptide by conjugating it with a polyethylene glycol (PEG, molecular weight = 3.4 kD) to enhance its hydrophilicity (8). The PEG was terminated with DOTA to chelate to ^{64}Cu . In this study, we characterized the binding affinity of this modified peptide to the FPR and determines its functional ability to detect neutrophils. Once we demonstrated that the peptide had the desired *in vitro* properties, *in vivo* imaging was performed on a mouse model of pulmonary inflammation.

MATERIALS AND METHODS

All chemicals obtained commercially were of analytic grade and used without further purification. ^{64}Cu - CuCl_2 was purchased from Isotracer, Inc. The peptide *N*-cinnamoyl-phe-(D)-Leu-phe-(D)-Leu-phe-lys- CONH_2 (cFLFLFK CONH_2) was synthesized via a solid-phase Fmoc method by Biomolecular Research Facility at the University of Virginia, and the structure was confirmed by matrix-assisted laser desorption/ionization time-of-flight (MALDI-TOF) mass spectroscopy, as reported previously (9). Bifunctional *t*-butoxycarbonyl-protected PEG-succinimidyl ester (*t*-Boc-PEG-NHS; molecular weight, 3.4 kD) was obtained from Laysan Bio, Inc. 2,2',2'',2'''-(1,4,7,10-tetraazacyclododecane-1,4,7,10-tetrayl)tetraacetic acid (DOTA) was obtained from Macrocylics, Inc. *N*-hydroxysulfosuccinimide and 1-ethyl-3-[3-(dimethylamino)propyl]carbodiimide were purchased from Pierce. All other chemical reagents and solvents were obtained from Sigma-Aldrich. Semipreparative reversed-phase (RP) high-performance liquid chromatography (HPLC) was performed on a Varian system with an ABI Spetroflow 783 ultraviolet detector and a Bioscan Flow Count Radio-HPLC detector with an Apollo C18 RP column (5 μm , 250 \times 10 mm). The mobile phase changed from 40% solvent A (0.1% trifluoroacetic acid in 80% water) and 60% solvent B (0.1% trifluoroacetic acid in 80% aqueous acetonitrile)

to 100% solvent B at 30 min at a flow rate of 3 mL/min. MALDI-TOF mass spectroscopy analysis was performed on samples of peptide products at W.M. Keck biomedical mass spectrometry laboratory at the University of Virginia, and the data were obtained on a Bruker Daltonics system.

Human tumor necrosis factor- α (TNF- α) was procured from Perpotech, and fMLF was purchased from Sigma. Aliquots of both samples were taken (TNF- α , 10 U/mL, and fMLF, 10 mM) and stored at -20°C . For every assay the solutions were thawed to ambient temperature and freshly diluted with hepatic arterial (HA) buffer before use. Multiscreen high-throughput screening (HTS) with glass fiber filter (FC) 96-well plates, type C, with 1.2- μm glass filters were purchased from Millipore. Filtration from 96-well plates was performed under vacuum on a Brandel filtration device. The membranes from each well were collected by punching with the Millipore Multiscreen punching instrument. The radioactivity from ^{64}Cu -bound ligand was measured with either Minaxi (Packard), Autogamma 5000 series (Packard), or Wallac 1420 Wizard (Perkin-Elmer) γ -counters. Radioactivity was measured for 1 min per sample and was not corrected for decay.

Synthesis and Radiolabeling

cFLFLFK-PEG-*t*-Boc was prepared by incubating a mixture of cFLFLFK(NH_2) (10 mg, 10.6 μmol) dissolved in 2 mL of acetonitrile and *t*-Boc-PEG-NHS (30 mg, 8.8 μmol) dissolved in 2 mL of sodium borate buffer (0.1N, pH 8.5) overnight at 4°C . Removal of volatiles under reduced pressure using a rotary evaporator afforded a residue that was dissolved in 2 mL of trifluoroacetic acid and left at room temperature for 2 h to remove the *t*-Boc protecting group. Concentration of the mixture under reduced pressure followed by reconstitution in 50% acetonitrile:water (2.0 mL) yielded stock solution. This solution was subjected to multiple injections (~5–6) on semipreparative RP HPLC to collect fractions containing pure cFLFLFK-PEG- NH_2 (retention time, 18.4 min.). The fractions were concentrated under reduced pressure to yield pure sample, which was further characterized by MALDI-TOF mass spectroscopy. The average molecular weight distribution of cFLFLFK-PEG- NH_2 was centered at 4.3 kD, and major *m/z* peaks were observed at 4240, 4284, 4372, and 4416. The average calculated mass was 4331.

cFLFLFK-PEG- NH_2 (16.5 mg, 3.8 μmol) was dissolved in 1 mL of H_2O , and the pH was adjusted to 8.5 with 0.1N NaOH. To this solution was added DOTA-NHS (19 μmol in 20 μL of water), prepared according to a previously reported method (9). The mixture was incubated overnight at 4°C . The solution was subjected to HPLC purification (retention time, 16.8 min.) to yield pure cFLFLFK-PEG-DOTA (7.6 mg, 43%). Characterization of the peptide by MALDI-TOF revealed an average molecular weight distribution centered at 4.8 kD, and major *m/z* peaks were observed at 4644, 4688, 4776, and 4820. The average calculated mass was 4718.

The radiolabeling was accomplished by addition of 7.4–29.6 MBq (200–800 μCi) of $^{64}\text{CuCl}_2$ to 5–20 μg of cFLFLFK-PEG-DOTA in 0.1N ammonium acetate (pH 5.5) buffer, and the mixture was incubated at 40°C for 30 min. The mixture was injected as is for RP HPLC purification. The column eluate was monitored by ultraviolet absorbance at 215 nm and with a γ -detector. The collected product eluted at 17.2 min with a radiochemical yield higher than 95% and a specific activity of 1.1×10^6 MBq/mmol (yield > 90%). Pure fractions were concentrated under reduced pressure. The radiolabeled peptide was further

characterized by comparing its chromatographic properties with nonradioactive copper-labeled compound synthesized independently using copper chloride in the same process. Analysis by MALDI-TOF revealed an average molecular weight distribution of about 4.8 kD, and major m/z peaks were observed at 4692, 4736, 4778, and 4794. The average calculated mass was 4782, which is in strong agreement with experimental values.

To test for compound stability, we incubated the compound in serum at 37°C for 1, 3, and 6 h. After incubation, we monitored the compound with HPLC. To determine the partition coefficient of the pegylated and nonpegylated compound, we dissolved about 350 kBq of cFLFLFK-PEG-DOTA-⁶⁴Cu (or cFLFLFK-DOTA-⁶⁴Cu) in 500 μ L of water and mixed the solution with 500 μ L of octanol in an Eppendorf microcentrifuge tube. The tube was sonicated for 10 min and then was centrifuged at 4,000 rpm for 5 min (Fisher Scientific Marathon Micro-A). Radioactivity was measured in 100- μ L aliquots of both octanol and water layers in triplicate.

In Vitro Assays

Receptor Binding. Human neutrophils were prepared from normal heparinized (10 U/mL) venous blood by a 1-step Ficoll-Hypaque separation procedure (10,11), yielding approximately 98% neutrophils; greater than 95% viable as determined with trypan blue containing less than 50 pg·mL⁻¹ of endotoxin. After separation, neutrophils were washed with Hanks' balanced salt solution with heparin (10 U/mL) 3 times. After the third wash, neutrophils were resuspended in HA buffer, which was Hanks' balanced salt solution supplemented with 0.1% human albumin (Bayer Healthcare). Neutrophil experiments were completed in HA buffer.

Freshly isolated human neutrophils (4×10^6 cells/mL) were treated with 10 U/mL of TNF- α -(Peprotech) 20 min before binding studies and transferred to a 96-well plate (Multiscreen HTS FC [Millipore] 1.2- μ m glass filter type C, 50.0 μ L, $\sim 2.0 \times 10^5$ cells per well). Saturation assays were performed using 8 different concentrations of cFLFLFK-PEG-⁶⁴Cu (specific activity, 5,143 MBq [139 mCi]/ μ g or 32.9 MBq [0.89 μ Ci]/mmol) ranging from 0.001 to 100 nM. Neutrophils were incubated with the radioligand at 25°C for 90 min to obtain total binding. After incubation, 96-well plates were filtered rapidly under a vacuum using a Brandel filtration device (Brandel Inc.), washed 3 times with cold Tris-Mg buffer (-5°C, 10 mM, 150 μ L each time per well) to remove the unbound radioligand, and dried under a vacuum. The membranes from each well were collected by the Millipore Multiscreen punching instrument. The bound radioactivity remaining on the membranes was measured in a γ -counter. Specific binding was calculated as the difference between total binding and nonspecific binding. Nonspecific binding was assessed using the highest concentration of radiolabeled ligand applied in the binding experiment after preincubation with cold compound (100 μ M of cFLFLFK-PEG-Cu). Binding parameters (K_d and B_{max} values) were calculated using PRISM 4.0 (GraphPad).

Superoxide Production Assay. The biologic activity of cFLFLFK-PEG-copper or fMLP was assessed by measuring the stimulated release of superoxide by neutrophils after exposure to a range of concentrations. The neutrophil oxidative activity (luminol-enhanced chemiluminescence) was measured using a microtitre polymorphonuclear chemiluminescence assay (11). Activated neutrophils emit light from unstable high-energy oxygen species produced by the plasma membrane-associated reduced nicotin-

amide adenine dinucleotide phosphate oxidase and release myeloperoxidase from primary granules. The light signal from activated neutrophils can be enhanced by the addition of luminol to the samples. Luminol-enhanced emission of light is stimulated by singlet oxygen, a reactive oxygen species, dependent on both the production of superoxide and mobilization of myeloperoxidase (12).

To prime the polymorphonuclear cells, purified cells (2×10^6 mL) were incubated in a water bath (37°C) for 15 min with TNF- α (10 U/mL). After priming, aliquots of the polymorphonuclear cells were transferred to a microtitre plate (white-walled clear bottom 96-well tissue culture plates) containing luminol (100 μ M) and (0.0001–10 μ M) cFLFLFK-PEG-Cu or fMLP. Peak stimulated chemiluminescence was determined with a Victor 1420 Multilabel Counter set for chemiluminescence mode using Wallac Workstation software. Sigmoidal dose-response curves for fMLP and cFLFLFK-PEG-Cu stimulation of polymorphonuclear oxidative activity were fit using PRISM 4.0 (GraphPad). Median effective concentrations (EC50) were derived from concentration-response curves using PRISM software. We compared relative agonist potency (EC50) of cFLFLFK-PEG-Cu to fMLP on polymorphonuclear oxidative activity.

In Vivo Assays

Lung Inflammation Model. *Klebsiella pneumoniae* strain 43816, serotype 2 (American Type Culture Collection), was grown in trypticase soy broth overnight, then subcultured for 2 h to log-phase growth. After extensive rinsing, bacteria were diluted in sterile normal saline for inoculation. C57BL/6 mice (male, 8–10 wk old; Charles River) were inoculated by oropharyngeal aspiration of 50 μ L of bacterial suspension (approximately 3×10^5 colony-forming units) under light inhalational anesthesia with methoxyflurane. The size of the inoculum was quantitated by plating serial dilutions on MacConkey agar plates and counting colony-forming units after overnight incubation. Mice showed signs of moderate illness 18–36 h after inoculation, when imaging was performed.

Organ Distribution and Pharmacokinetics. Distribution of radioactivity in the body was determined in both control ($n = 4$) and *Klebsiella*-infected ($n = 6$) mice 18 h after injection of cFLFLFK-PEG-⁶⁴Cu. After a single blood sample had been taken from the tail vein, mice were euthanized by deep halothane anesthesia. The pulmonary circulation was flushed with 3 mL of sterile normal saline via the right ventricle and the following organs and tissues were removed and washed: heart, lungs, muscle, bone, liver, kidney, spleen, small intestine, and stomach. The dissected tissues were placed in a preweighed vial and later assayed in a γ -well counter. The measured radioactivity for each sample was decay-corrected back to the time of tracer injection. Biodistribution values are expressed as a percentage of the injected dose (%ID) and normalized for body and organ/tissue mass (13).

Blood kinetics of cFLFLFK-PEG-⁶⁴Cu were studied in 3 control mice. Approximately 50 μ L of blood from the contralateral tail vein were collected in capillary tubes at 5, 15, 30, 60, 120, and 180 min after tracer injection (0.37–0.74 MBq). The capillary tubes were placed in a vial that was weighed beforehand and afterward. Activity in each blood sample was measured in a γ -counter, normalized for injected dose and animal body weight, and expressed as %ID/g of blood.

Myeloperoxidase Analysis. To estimate the number of intrapulmonary neutrophils, myeloperoxidase assays were performed.

Immediately after being imaged, mice were euthanized by deep halothane anesthesia and their pulmonary circulation flushed with 3 mL of sterile normal saline via the right ventricle. The lungs were removed and snap frozen at -80°C until later assayed. Lungs were weighed and placed in homogenization buffer (hexadecyltrimethylammonium bromide) and homogenized, followed by sonication and centrifugation. Five microliters of supernatant were added to the assay buffer (o-dianisidine hydrochloride in potassium phosphate) in a 96-well plate, and optical density kinetic measurements at wavelength 490 were made using a μQuant (Bio-Tek Instruments, Inc.) spectrophotometer. Myeloperoxidase activity is reported as a change in optical density (OD)/min/mg of lung tissue.

Lung Immunohistochemistry Staining

Immunohistochemical analysis was performed on harvested lung tissue 42 h after *Klebsiella* administration, which matches the time point of imaging after infection (24 h plus an additional 18 h of tracer clearance time). Immunohistochemistry was used to assess the relative amount and distribution of neutrophils, compared with macrophages, in the lungs of control versus infected mice. Before removal of the lungs, the pulmonary circulation was flushed with saline via the right ventricle to eliminate nonadherent white blood cells. The lungs were then inflated with formalin to distend the alveolar spaces uniformly. The trachea was cannulated, and 10% phosphate-buffered formalin was infused at a pressure of 25 cm of H_2O . After fixation, the lung was dissected coronally in the plane of the mainstem bronchus. Adjacent histologic sections (3 μm thick) were specifically stained for either neutrophils with a monoclonal rat antimouse neutrophil IgG (MCA771G; Serotec) or for macrophages with anti-MAC-2 IgG (ACL8942P; Accurate). Stained cells were observed under a light microscope (Microphot; Nikon, LRI Instruments AB).

PET/CT Study

Imaging Protocol. Twenty-four hours after administration of *Klebsiella pneumoniae*, cFLFLFK-PEG- ^{64}Cu (3.7–5.5 MBq [(~ 100 – 150 μCi)] in 200 μL of saline was injected via the tail vein. Lung standardized uptake values (SUVs) were measured at several time points after injection and fit to a monoexponential curve, allowing for the calculation of ligand clearance in the control and infected lungs. This analysis provides us with an estimate of the time window after injection for which the signal difference between control and infected lungs is maximized.

For accurate image coregistration, mice were placed prone in a custom-designed portable imaging tray, facilitating precise positioning between scanners. Anesthesia (1%–2% isoflurane in oxygen) was delivered throughout the imaging. Micro-CT (14) images were acquired using a scanner developed in-house. After CT acquisition, the mice were transported to the small-animal PET scanner (Focus F-120; Siemens) and scanned for approximately 25 min. CT images were reconstructed with a 3-dimensional filtered backprojection algorithm using the COBRA software (Exxim, Inc.). The reconstructed pixel size was $0.15 \times 0.15 \times 0.15$ mm on a $320 \times 320 \times 384$ image matrix. Using microPET Manager (version 2.4.1.1; Siemens), PET data were reconstructed using the OSEM3D/MAP algorithm (zoom factor, 2.164). The reconstructed pixel size was $0.28 \times 0.28 \times 0.79$ mm on a $128 \times 128 \times 95$ image matrix. All small-animal PET images were corrected for decay but not attenuation.

Image Analysis. PET and CT images were coregistered using ASIPRO (Siemens) and a transformation matrix previously obtained with an imaging phantom. To characterize the accumulation of the tracer in lungs, region-of-interest (ROI) analysis was performed. CT images were used to visualize lung boundaries and guide the placement of lung ROIs, which were drawn manually. Ten ± 2 contiguous transaxial lung ROIs were drawn to cover the entire lung volume. Lung ROIs were transferred to the PET images, and the mean activity per milliliter of lung tissue was determined. SUVs, defined as the product of the mean lung ROI activity and the animal body weight divided by the injected dose, were computed.

Data Analysis

Group data are expressed as the mean \pm SD. The Student *t* test was used to determine differences in SUV, %ID, and myeloperoxidase results among mice administered *Klebsiella pneumoniae* and normal control mice. A *P* value of less than 0.05 indicated statistical significance. Sigma-Stat, version 3.0 (SPSS, Inc.), was used for statistical calculations.

RESULTS

Peptide Synthesis and Radiolabeling

The desired cFLFLFK-PEG-DOTA peptide containing a PEG linker was synthesized in a straightforward manner using a standard synthesis protocol of activating the carboxylic acid group on *t*-Boc protected-PEG with *N*-hydroxysuccinimide derivatization. Deprotection of *t*-Boc on PEG linker with trifluoroacetic acid afforded a pegylated peptide with free NH_2 , which was further acylated with an *N*-hydroxylated-carboxy derivative of DOTA. At each step, the intermediates were purified by RP HPLC and the compounds were characterized by MALDI-TOF mass analysis. The final radiolabeled cFLFLFK-PEG- ^{64}Cu ligand exhibited a pure single peak by RP HPLC chromatography, and its radio purity was assigned to be more than 95%. The radiolabeled compound was compared with its nonradioactive counterpart for additional confirmation of the structure. HPLC analysis yielded no free ^{64}Cu ions or radioligand fragments when testing the stability of the tracer in serum. The partition coefficients of cFLFLFK-PEG- ^{64}Cu and cFLFLFK- ^{64}Cu were measured to be -1.21 and 1.25 , respectively, indicating the effectiveness of the PEG in enhancing the compound's water solubility.

In Vitro Assays

The binding assay of the cFLFLFK-PEG- ^{64}Cu to freshly purified human neutrophils yielded a mean K_d value of 17.7 nM. A representative saturation curve of specifically bound cFLFLFK-PEG- ^{64}Cu is shown in Figure 1. The binding data are additionally shown as a Scatchard plot in Figure 1. cFLFLFK-PEG- ^{64}Cu showed minimal agonist activity as assessed by neutrophil superoxide production at all concentrations studied, whereas fMLF displayed agonist activity with an EC_{50} of 5.1×10^{-7} M (Fig. 2).

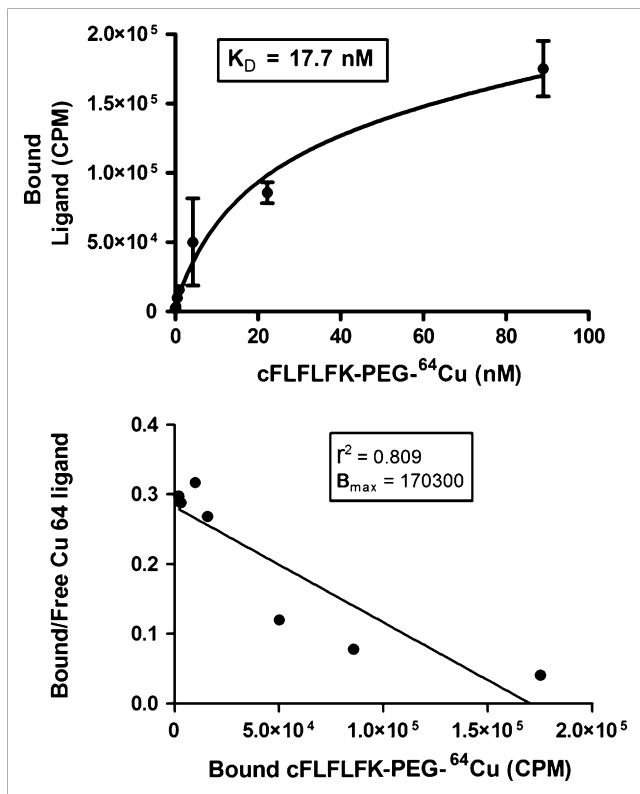


FIGURE 1. Representative saturation curve of cFLFLFK-PEG-⁶⁴Cu specifically bound to human neutrophils. Binding affinity was computed to be 17.7 nM. Binding data have also been plotted as Scatchard plot. Nonspecific binding was computed in presence of excess cold compound and is estimated to contribute to 20%–30% of total binding.

In Vivo Assays

Blood Kinetics. The clearance of cFLFLFK-PEG-⁶⁴Cu in blood followed a monoexponential elimination pattern. The mean biologic half-life of the peptide was calculated to be 55 ± 8 min.

Organ Distribution. Excised tissue concentrations of radiotracer (%ID) at 18 h after injection in controls and mice administered *Klebsiella pneumoniae* are shown in Figure 3. For *Klebsiella*-infected mice, the highest mean concentrations were found in the liver, kidney, and small intestine. The following organs (or tissue) demonstrated statistically significant differences in mean %ID values between control and infected mice as determined by Student *t* test: heart, lungs, liver, kidney, small intestine, stomach, and blood. Muscle, bone, and spleen did not exhibit statistically significant differences at the time point observed. The mean ratio of radioactivity in the infected to control lungs was 3.8.

Imaging Results. The imaging properties of cFLFLFK-PEG-⁶⁴Cu were studied in control ($n = 4$) and *Klebsiella*-infected ($n = 6$) mice. To establish the optimal time for imaging after ligand injection, the rate of washout in the control and infected lungs was computed. The ligand half-

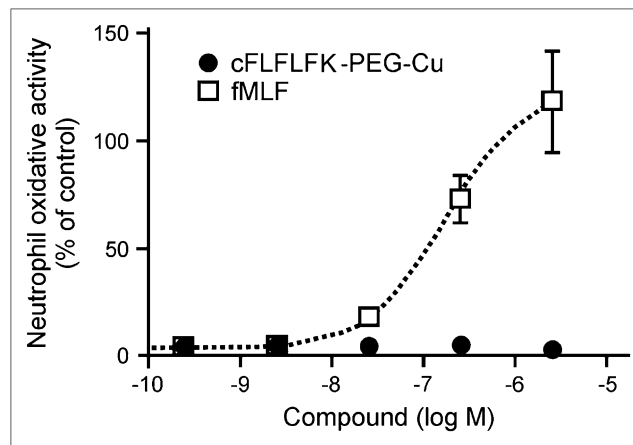


FIGURE 2. Stimulation of neutrophil oxidative burst by cFLFLFK-PEG-Cu and fMLF as detected by luminol-enhanced chemiluminescence. Results are reported as peak chemiluminescence as percentage of TNF-primed and fMLF-stimulated (10^{-6} M) control. cFLFLFK-PEG-Cu demonstrated no agonist activity toward neutrophils (EC₅₀ value not computable), whereas fMLF stimulated neutrophil superoxide release with EC₅₀ of 3.7×10^{-7} M. Data are reported as mean \pm SEM for at least 2 independent measurements.

life was determined to be 4.8 ± 0.7 h in the control lung and 10.3 ± 2.9 h in the infected lung. From these clearance half lives, the optimal imaging time window after injection was determined to be between 14 and 20 h. The 18-h time point was chosen for convenience. Figure 4 shows representative CT and PET images of cFLFLFK-PEG-⁶⁴Cu 18 h after injection. These images show significant tracer accumulation in the lungs of the *Klebsiella*-infected mouse, compared with the control mouse. Average lung SUVs for *Klebsiella*-infected and control mice were 0.142 ± 0.054 and 0.028 ± 0.003 , respectively ($*P < 0.003$), as shown in Figure 5. High liver uptake was observed in the PET images regardless of whether lung infection was present. The mean lung SUV ratio in infected versus control mice was approximately 5.8.

Myeloperoxidase Analysis. Myeloperoxidase values measured in excised lung tissue (after imaging) revealed significantly elevated enzyme activity in mice administered *Klebsiella pneumoniae*, compared with controls (Fig. 6). Mean myeloperoxidase assay values (measured in change in optical density/min/mg of lung tissue) for *Klebsiella*-infected and control mice were 0.78 ± 0.17 and 0.12 ± 0.05 , respectively ($*P < 0.005$). The ratio of mean myeloperoxidase activity in the infected to the control lungs was 6.3, slightly higher than the mean lung SUV ratio measured in the same mice.

Lung Immunohistochemistry Staining. Immunohistochemical staining of lung tissue from a control mouse revealed very few neutrophils (Fig. 7A) or macrophages (Fig. 7B), and a normal alveolar wall structure. In contrast, the *Klebsiella*-infected mouse (euthanized 42 h after ad-

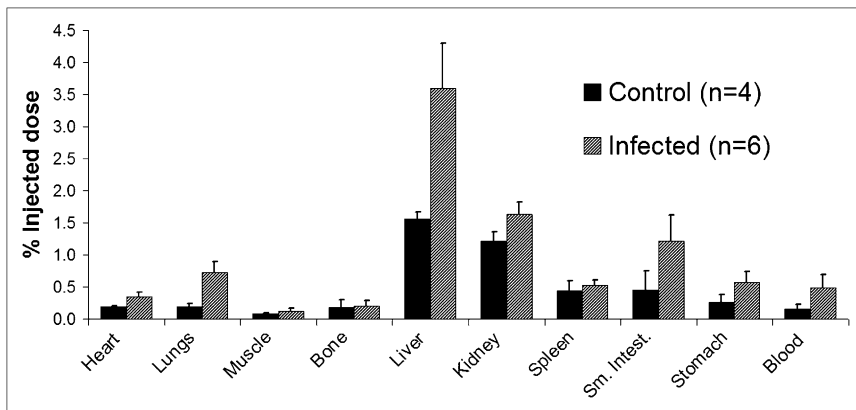


FIGURE 3. Tissue and organ accumulation of cFLFLFK-PEG-⁶⁴Cu at 18 h after injection in control and *Klebsiella*-infected mice, expressed as %ID/g of tissue. Mean lung radioactivity is 3.8 times greater in infected lungs than in control lungs (**P* < 0.05).

ministration) had a significant lung neutrophil burden (Fig. 7C), with very low numbers of macrophages (Fig. 7D).

DISCUSSION

Although chemotactic peptide receptor agonists have been used successfully in numerous animal studies (5),

they are not suitable inflammation imaging reagents because of their potential influence on leukocyte biologic function. It has been previously demonstrated that the peptide cFLFLFK has a high binding affinity toward the neutrophil FPR and possesses antagonistic properties and thus does not induce neutropenia as do other high-affinity chemotactic peptide analogs (3). Another advantage is that radiolabeling procedures for antagonist peptides may be simpler and require less controlled generator elution and HPLC purification because of their minimal induced biologic activity toward neutrophils. In this study, it was shown that the peptide cFLFLFK can be conjugated with a PEG for the purpose of enhancing its hydrophilicity without significantly altering its binding affinity toward the neutrophil FPR. Binding studies to human neutrophils revealed a K_d of 17.7 nM, suggesting that the pegylation of peptide does not significantly alter the binding affinity toward the FPR, when compared with unaltered parent peptide ($K_d = 2$ nM) as reported by Babich et al. (3). In addition, the modification of peptide by pegylation may offer the prospect of fine-tuning pharmacokinetic param-

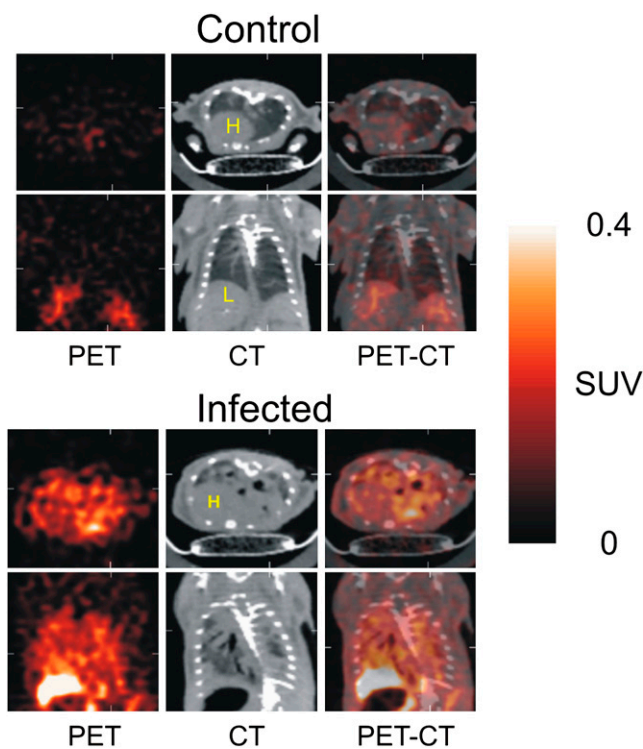


FIGURE 4. Examples of micro-CT and small-animal PET images of control and *Klebsiella*-infected mice. PET images were obtained 18 h after tail vein injection of cFLFLFK-PEG-⁶⁴Cu. Both transverse (top row) and coronal (bottom row) images are shown. In mice administered *Klebsiella*, there is extensive attenuation in lungs on CT scans, compared with controls. PET scans revealed that *Klebsiella*-infected mice had visually more tracer uptake in lung tissue than did controls, as was quantified by ROI analysis. Color bar along side indicates increasing tissue radioactivity on PET images. H = heart; L = liver.

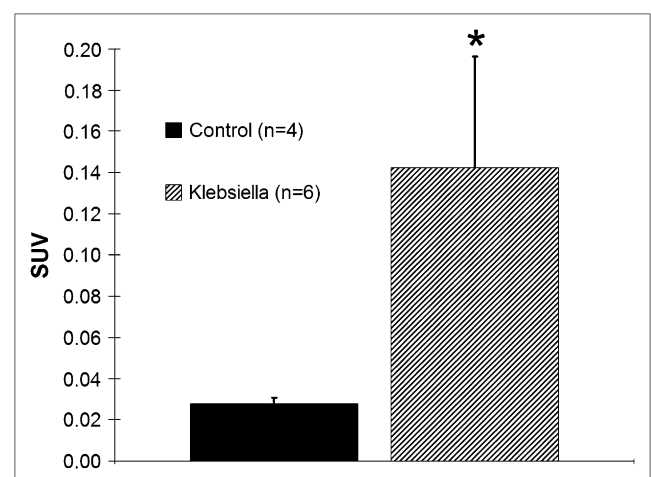


FIGURE 5. Lung SUVs for control and *Klebsiella*-infected mice. Lung SUVs were 5.8 times greater in *Klebsiella*-infected mice than in controls (**P* < 0.005).

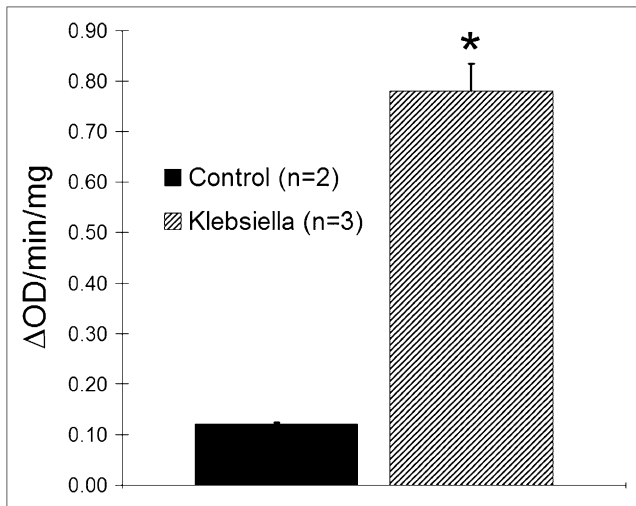


FIGURE 6. Myeloperoxidase activity in lung homogenates, expressed as change in optical density (15) per minute per milligram of tissue. Myeloperoxidase activity measured in *Klebsiella*-infected lungs was approximately 6-fold higher than that measured in control lungs (* $P < 0.05$). Δ OD = change in optical density.

ters of the ligand to improve bioavailability and clearance. Additionally, the compound cFLFLFK-PEG-⁶⁴Cu showed no biologic activity toward neutrophils as demonstrated by superoxide stimulation assays. In vivo biodistribution studies revealed high nontarget uptake in the liver, kidneys, and small intestine. Infected mice had significantly more tracer accumulation in liver and blood than did controls. This finding may be explained by elevated metabolism and enhanced recruitments of neutrophils in response to bacteria in the lungs. Blood clearance followed a monoexponential pattern.

SUV measurements confirmed that the localization of the peptide was significantly higher in the lungs of *Klebsiella*-infected mice than in controls at 18 h after injection. Even though the blood half-life may be approximately 1 h, the ligand does not clear from the lungs at this rate.

To verify that the increase in measured lung SUVs is primarily due to infiltrating neutrophils responding to the bacteria, we performed myeloperoxidase assays on postimaged lung tissue. Myeloperoxidase analysis confirmed an increased population of leukocytes in the infected lungs, the magnitude of which correlated well with our average SUV results. Because myeloperoxidase is an enzyme that is not exclusively found in neutrophils but is also found in macrophages, we sought additional evidence that neutrophils constitute the majority of infiltrating leukocytes in the lungs of this model. We assessed the relative amounts of neutrophils and macrophages in both control and infected lungs by immunohistochemical analysis, which revealed that the primary cells infiltrating the infected lungs at the 42-h time point after *Klebsiella* administration were neutrophils, with significantly fewer macrophages. We can

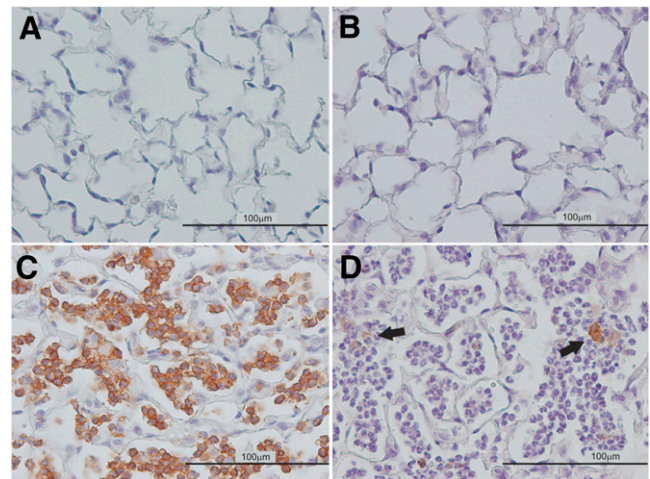


FIGURE 7. Immunohistochemical staining of neutrophils (stained with rat antimouse IgG [MCA771G; Serotec]) and macrophages (stained with anti MAC-2 IgG [ACL8942P; Accurate]) in lung tissue excised from control and *Klebsiella*-infected mouse (42 h after administration). Immunostained cells appear dark brown. Control lungs revealed no neutrophils (A) or macrophages (B), only normal alveolar wall structure. Infected lungs had significant neutrophil accumulation (C), with little macrophage infiltration (D, indicated by arrows). (Magnification, $\times 400$.)

therefore attribute our elevated lung SUV measurements in *Klebsiella*-infected mice to infiltrating neutrophils, as is consistent with results reported by other groups (15).

Micro-CT scans demonstrated significant changes in lung tissue characteristics as a result of administration of *Klebsiella pneumoniae*. Figure 4 exemplifies the marked increase in lung density that takes place 42 h after infection. Although CT is sensitive to changes in lung tissue density, it cannot distinguish inflammation from fibrosis or edema, nor can it be used to identify which type of inflammatory cell is predominantly infiltrating the lungs.

CONCLUSION

We have demonstrated that the bioavailability and blood clearance properties of the peptide ligand cFLFLFK can be improved by conjugation with a PEG-modified linker without adversely affecting its binding affinity or antagonistic properties toward the FPR on neutrophils. We also demonstrated that imaging of acute inflammation can be achieved with this newly designed peptide with improved pharmacodynamic parameters and that the mechanism by which the compound accumulates appears to be through binding to receptors on neutrophils. Further biologic evaluation of this novel imaging agent is ongoing, with the goal of refining the biologic properties of the agent to facilitate studies that assess the efficacy of novel antiinflammatory therapeutic drug candidates. On the basis of in vivo imaging results and in vitro cell function assays, this peptide appears to be a promising new radiopharmaceutical for the in vivo imaging of neutrophils.

ACKNOWLEDGMENTS

This research was supported by the Commonwealth Foundation for Cancer Research, NIH grants HL-073361 and HD-051609, and a gift provided by Philip Morris USA (The review and approval process was overseen by an External Advisory Committee without any affiliation with the University, PMUSA, or any other tobacco company. PMUSA funding for this work to SSB was based upon independent intramural and extramural reviews). The following people contributed to this work: Joe Pole, Mark Williams, and Ge Gao.

REFERENCES

1. Eruslanov EB, Lyadova IV, Kondratieva TK, et al. Neutrophil responses to Mycobacterium tuberculosis infection in genetically susceptible and resistant mice. *Infect Immun*. 2005;73:1744–1753.
2. Thakur ML, Lavender JP, Arnot RN, Silvester DJ, Segal AW. Indium-111-labeled autologous leukocytes in man. *J Nucl Med*. 1977;18:1014–1021.
3. Babich JW, Dong Q, Graham W, et al. A novel high affinity chemotactic peptide antagonist for infection imaging [abstract]. *J Nucl Med*. 1997;38(suppl):268P.
4. Fischman AJ, Pike MC, Kroon D, et al. Imaging focal sites of bacterial infection in rats with indium-111-labeled chemotactic peptide analogs. *J Nucl Med*. 1991;32:483–491.
5. Babich JW, Tompkins RG, Graham W, Barrow SA, Fischman AJ. Localization of radiolabeled chemotactic peptide at focal sites of Escherichia coli infection in rabbits: evidence for a receptor-specific mechanism. *J Nucl Med*. 1997;38:1316–1322.
6. vander Laken CJ, Boerman OC, Oyen WJG, et al. Technetium-99m-labeled chemotactic peptides in acute infection and sterile inflammation. *J Nucl Med*. 1997;38:1310–1315.
7. Derian CK, Solomon HF, Higgins JD, et al. Selective inhibition of N-formylpeptide-induced neutrophil activation by carbamate-modified peptide analogues. *Biochemistry*. 1996;35:1265–1269.
8. Chen X, Hou Y, Tohme M, et al. Pegylated Arg-Gly-Asp peptide: ⁶⁴Cu labeling and PET imaging of brain tumor $\alpha\text{v}\beta_3$ -integrin expression. *J Nucl Med*. 2004;45:1776–1783.
9. Zhang Y, Kundu B, Fairchild KD, et al. Synthesis of novel neutrophil-specific imaging agents for positron emission tomography (PET) imaging. *Bioorg Med Chem Lett*. 2007;17:6876–6878.
10. Ferrante A, Thong YH. Simultaneous preparation of mononuclear and polymorphonuclear leucocytes from horse blood on Ficoll-Hypaque medium. *J Immunol Methods*. 1980;34:279–285.
11. Sullivan GW, Rieger JM, Scheld WM, Macdonald TL, Linden J. Cyclic AMP-dependent inhibition of human neutrophil oxidative activity by substituted 2-propynylcyclohexyl adenosine A(2A) receptor agonists. *Br J Pharmacol*. 2001;132:1017–1026.
12. Dechatelet LR, Long GD, Shirley PS, et al. Mechanism of the luminol-dependent chemi-luminescence of human-neutrophils. *J Immunol*. 1982;129:1589–1593.
13. Baker HC. Lindsey Ri, Weisbroth SH. *The Laboratory Rat*. New York, NY: Academic Press; 1980.
14. Handl HL, Vagner J, Han H, Mash E, Hraby VJ, Gillies RJ. Hitting multiple targets with multimeric ligands. *Expert Opin Ther Targets*. 2004;8:565–586.
15. Zhou Z, Kozlowski J, Goodrich AL, Markman N, Chen DL, Schuster DP. Molecular imaging of lung glucose uptake after endotoxin in mice. *Am J Physiol Lung Cell Mol Physiol*. 2005;289:L760–L768.